

OPEN ACCESS

Diagonalizing sensing matrix of broadband RSE

To cite this article: Shuichi Sato *et al* 2006 *J. Phys.: Conf. Ser.* **32** 072

View the [article online](#) for updates and enhancements.

Related content

- [Experimental investigation of a control scheme for a tuned resonant sideband extraction interferometer for next-generation gravitational-wave detectors](#)
F Kawazoe, S Sato, V Leonhardt *et al.*
- [Length sensing and control for Einstein Telescope Low Frequency](#)
Vaishali Adya, Sean Leavey, Harald Lück *et al.*
- [Development of a signal-extraction scheme for resonant sideband extraction](#)
K Kokeyama, K Somiya, F Kawazoe *et al.*

Recent citations

- [Diagonalization of the length sensing matrix of a dual recycled laser interferometer gravitational wave antenna](#)
Seiji Kawamura *et al*
- [The Experimental plan of the 4m Resonant Sideband Extraction Prototype for The LCGT](#)
F Kawazoe *et al*



240th ECS Meeting ORLANDO, FL
Orange County Convention Center Oct 10-14, 2021



Abstract submission due: April 9

SUBMIT NOW

Diagonalizing sensing matrix of broadband RSE

Shuichi Sato¹, Keiko Kokeyama², Fumiko Kawazoe², Kentaro Somiya³ and Seiji Kawamura¹

¹TAMA project, National Astronomical Observatory of Japan, 2-21-1 Osawa Mitaka, Tokyo, 181-8588, Japan

²The Graduate School of Humanities and Sciences, Ochanomizu University, 2-1-1, Otsuka, Bunkyo-ku, Tokyo 112-8610 Japan

³Max-Planck-Institut für Gravitationsphysik, Am Mühlenberg 1, 14476 Golm, Germany

E-mail: sato.shuichi@nao.ac.jp

Abstract. For a broadband-operated RSE interferometer, a simple and smart length sensing and control scheme was newly proposed. The sensing matrix could be diagonal, owing to a simple allocation of two RF modulations and to a macroscopic displacement of cavity mirrors, which cause a detuning of the RF modulation sidebands. In this article, the idea of the sensing scheme and an optimization of the relevant parameters will be described.

1. Introduction

First generation gravitational wave (GW) antennas are currently going on line to search for gravitational waves. At the same time, significant effort is dedicated to R&D for the next generation GW antennas, such as Advanced LIGO in the U.S., and LCGT in Japan. These second generation GW detectors will employ an optical configuration called “resonant sideband extraction” (RSE)[1], which is one of the operation modes of a Dual Recycled Fabry-Perot Michelson Interferometer (DRFPMI). Dual recycling is a combination of power- and signal-recycling schemes, which is realized by adding a signal recycling mirror to the power-recycled FPMI (PRFPMI) between the beam splitter and the dark port, as is shown in Figure 1. The

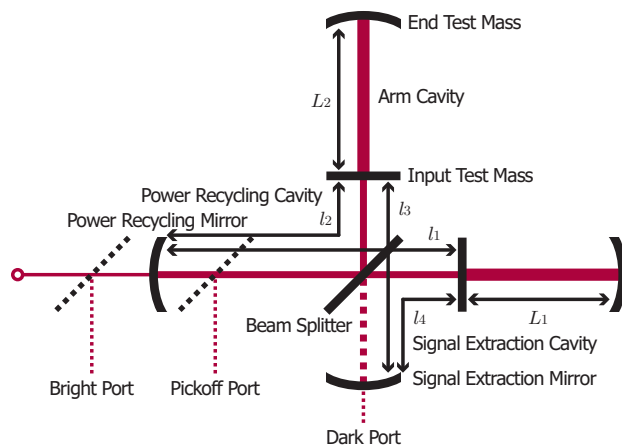


Figure 1. The schematic of the RSE interferometer optical configuration. The length degrees of freedom and the signal extraction ports are also defined in addition to the optical arrangement, and cavity lengths. The signal extraction mirror is placed between the beamsplitter and the dark port to enhance the detector response, which make the whole interferometer system more complex.

laser light resonates inside both arm cavities and the power recycling cavity, which is the same as first generation GW detectors now employing the PRFPMI configuration. For the PRFPMI configuration, for example, which is a baseline optical configuration for TAMA300, Initial-LIGO and VIRGO detector, the total number of longitudinal (cavity length) degrees of freedom to be controlled is four; common and differential length of the arm cavities, power-recycling cavity (PRC) length and Michelson differential length. In order to extract the four sensing signals, a single RF phase modulation is applied and three signal extraction ports (bright, dark and pickoff ports) are used for sensing. On the other hand, the DRFPMI/RSE configuration have five length degrees of freedom to be controlled in connection with the additional SEM, as shown in Table 1. The addition of the extra mirror makes the main interferometer more complex; it becomes a

Table 1. The definitions of the length degrees of freedom.

Name	Symbol	Definition	Derivative
Common arm length	L_+	$L_1 + L_2$	δL_+
Differential arm length	L_-	$L_1 - L_2$	δL_-
PRC length	l_P	$l_1 + l_2$	δl_P
Michelson length	l_-	$l_1 - l_2$	δl_-
SEC length	l_S	$l_3 + l_4$	δl_S

double coupled cavity system, which consists of arm cavities, a power-recycling and a signal-recycling (extraction) cavity all connected with a Michelson interferometer (MI). Toward the firm realization of this advanced optical configuration, there were several table-top experiments performed using the RSE system to study sensing and control methods, and to demonstrate the feasibility of dual-recycling with FP cavities; [2] [3][4][5]. These are all for detuned operation of RSE, especially for advanced LIGO, and a prototype experiment at the 40m interferometer at California Institute of Technology is now in progress [6].

The core of the sensing scheme is a sensing matrix; the primary goal is to extract the five error signals independently without a signal mixture of other degrees of freedom. It is clear that a diagonalized sensing matrix is absolutely advantageous for a robust control of the complicated interferometer systems and also for a cross-coupling noise issue, which arise from multi-path feedback loops. In addition, some merit could be also expected for the lock acquisition issue. So the development of the length sensing and control scheme, which gives a diagonal sensing matrix, was vigorously promoted especially for use in broad-band RSE systems. In this paper, the emphasis is placed on description of a sensing scheme which results in a diagonal sensing matrix, and an optimization of the optical configuration parameters of RSE using both analytical and numerical simulation ¹.

2. Diagonalizing the sensing matrix

The sensing scheme is associated one-on-one with the usage of the RF modulation(s); the number of the modulations, the resonance conditions of the modulations inside cavities and Schnupp asymmetry factor. Then secondary, actual modulation frequencies and the cavity lengths can be determined appropriately. The concepts of the suggested signal extraction scheme can be consolidated in the following two points;

- A very simple allocation of two sets of modulation sidebands; The PM ² sidebands are

¹ The numerical simulation was performed using FINESSE simulation software. [7]

² PM: phase modulation, AM: amplitude modulation.

completely transmitted by the MI³ and resonate inside the PRC+SEC,⁴ in contrast, a set of AM sidebands is completely reflected by the MI, and resonates only inside the PRC.

- Equal macroscopic displacement of the PRM and SEM will cause the detuning of AM only.

By imposing these conditions, the length sensing matrix becomes almost diagonal with five error signals, which are sensitive to each of the five degrees of freedom. In the following, more details of the concept, and a practical realization of the idea will be described.

2.1. General description on the signal sensing of the RSE interferometer

Before going to the essential points, a general description is given for the short review on the signal sensing issue, which clearly exposes an intrinsic difficulty. As it is shown in previous works, the sensing signals for common and differential arm cavities length are big enough compared with l_x signals, because the phase sensitivity of the arm cavities are enhanced by its high finesse. This means that L_+ and L_- signals can be extracted relatively cleanly, without significant mixture of the signals from other degrees of freedom. So the issue now is that how the remaining three signals l_P , l_- , l_S (collectively referred to as l_x signals) of the central interferometer part can be extracted. These difficulties essentially come from the following facts;

- The carrier field of the laser resonates and is enhanced inside the arm cavities to have maximum phase sensitivity to the length change of the arm cavities, so the carrier has a lot of information about the L signals. Thus it is quite difficult to extract l_x signals cleanly from the beat between carrier and the phase-modulated sidebands using PDH[8] method.
- The power recycling and signal recycling cavities are connected serially through a Michelson interferometer, whereby, both error signals for l_P and l_S appear in same demodulation phase.

As for the first term, a double RF modulation scheme was suggested[3] to avoid significant mixture of the arm cavity signals. Two sets of sidebands do not resonate inside the arm cavities and circulate differently inside DRMI to produce PD signals. This is called the double-modulation/double-demodulation scheme. In the second, if one concentrates on the central interferometer which consists of the input test masses, two recycling mirrors and beam splitter, DRMI can be regarded as a type of coupled cavity. Thus the issue is now reduced to the signal extraction for a coupled cavity as far as the signal separation of l_P and l_S is concerned.

2.2. Allocation of two modulations

One of the RF modulations (mod-1) should be present at the dark port to serve as a local oscillator for a carrier field on demodulation process at GW signal read out port, so it has to be a phase modulation (PM). On the other, another modulation (mod-2) should be an amplitude modulation (AM) in order to produce error signals with the beating between mod-1 and mod-2, for the broadband-operated RSE. Consider following modulation design to satisfy above conditions most efficiently;

- mod-1(PM) resonates both inside PRC and SEC to reach the dark port.
- The mod-1 pass through the MI completely: $\alpha_1 = \pi/2 + n\pi$ ⁵
- The mod-2 circulates only inside PRC, acting as a local oscillator on a double-demodulation process with the mod-1 to produce l_S signal efficiently
- The mod-2 is completely reflected by the MI: $\alpha_2 = n'\pi$

³ MI: Michelson Interferometer, consists of beam splitter and two input test masses.

⁴ PRC: power-recycling cavity, SEC: signal extraction cavity

⁵ The sideband behavior at MI is determined by the Schnupp asymmetry factor $\alpha_i = l_{sch}\omega_i/c$, where l_{sch} is a Schnupp asymmetry and ω_i is a i-th modulation frequencies. The reflectivity of the MI is defined as $\cos \alpha_i$, and the transmissivity as $\pm \sin \alpha_i$ when the Michelson fringe was controlled so as the dark port is dark for the carrier light.

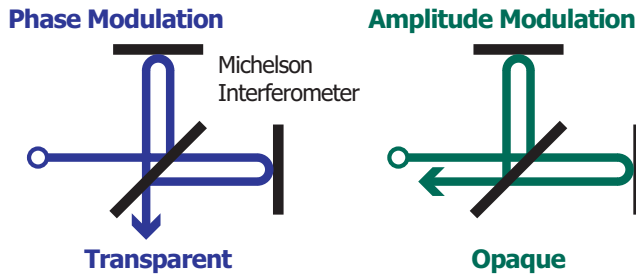


Figure 2. The Schnupp asymmetry designs for both modulations. The phase modulation mod-1 transmits through the MI completely, so the MI act as a simple steering mirror, meanwhile, the amplitude modulation mod-2 is reflected by the MI completely, so the MI act as an ideal reflecting mirror.

These conditions are illustrated in Fig 2. The arm cavity signals, L_+ and L_- , are extracted from the conventional single demodulation with the carrier and the mod-1 phase modulation in relatively independent way, whereas, l_x signals for the central part of the RSE are expected to arise from double-demodulation using mod-1 and mod-2. Under these conditions, however, l_P and l_S signals appear in an exactly same demodulation phase, which means that these two signals are completely degenerate. This is a nature of the coupled cavity system, so the issue is fully essential.

2.3. Delocation : The detuning of the modulation sidebands

The idea to resolve this degeneracy is that two error signals might be moved into separate demodulation phases by making one or both sideband fields off-resonant inside one or both cavities. This causes the rotation of the phase of the light fields, which leads to different optimum demodulation phase for two error signals. To realize this condition, a simple way is to make the cavity(ies) off-resonant with a macroscopic displacement of the cavity mirrors from original position. The microscopic cavity lengths have to be tuned for maintaining appropriate carrier resonance conditions, but the sideband fields are slightly detuned. This intentional off-resonance of sidebands is called “Delocation”, which is in other words, a macroscopic detuning. The phase modulation sidebands, mod-1, are local oscillator for GW signal readout, so it should be exactly resonant inside DRMI to avoid a possible noise coupling due to offset locking. Suppose mod-2 is delocated inside the power recycling cavity as is shown in Figure 3. A macroscopic displacement of the PRM is necessary to realize the detuning of mod-2, so the SEM must also be displaced by same amount to ensure the exact resonance of mod-1.

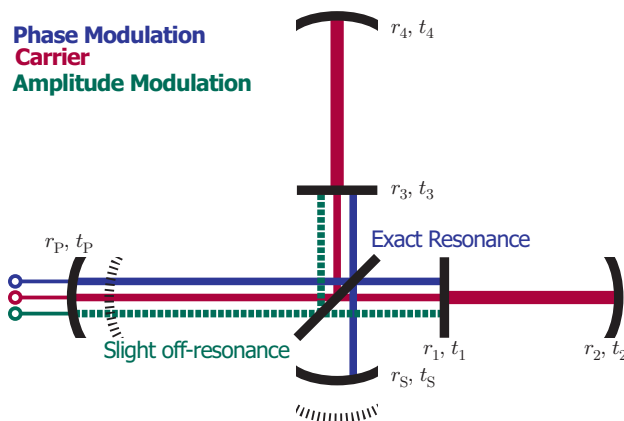


Figure 3. The allocation of the optical fields inside RSE interferometer and a “Delocation”. The carrier, a probe of the GW signal, is resonant inside the arm cavities and the PRC. One of the RF sidebands, mod-1, is a phase modulation and resonates both inside the PRC and the SEC to reach the dark port. On the other hand, the other sidebands, mod-2, act as a local oscillator for the double-demodulation process with mod-1, so it circulates only inside power-recycling cavity. A delocation makes only mod-2 slightly off-resonant inside PRC.

The signal sensitivities for l_P and l_S at the pickoff port are given analytically⁶ as

$$\begin{aligned}\frac{\partial V_P}{\partial l_P} &= g_{P1} r_{A1} \cos \delta_1 \Re \left[\left(g_{P1} r_S r_{A2} + g_{P2U} e^{-i\Delta_{P2}} \right) g_{P2U} e^{-i\delta_2} \right] \\ \frac{\partial V_P}{\partial l_S} &= g_{P1}^2 r_S r_{A1}^2 \cos \delta_1 \Re \left[g_{P2U} e^{-i\delta_2} \right]\end{aligned}$$

where, r_x is a mirror reflectivity (x: P for PRM and S for SEM), r_{yz} is a reflectivity of optical system y (y: A for arm cavity) for field z (z: 1 for mod-1, 2U for upper sideband of mod-2). g_{yz} is a cavity enhancement factor inside cavity y (y: P for PRC) for field z; for example, $g_{P1} = t_P / (1 - r_P r_S r_{A1}^2)$, $g_{P2U} = t_P / (1 + r_P r_{A1} e^{-i\Delta_{P2}})$. In addition, $\Delta_{yz} = 2l_{\Delta} \Omega_i / c$ is a delocation phase inside cavity y of the field x, which is a detuning phase of the sideband- i by a macroscopic displacement l_{Δ} . The δ_i are demodulation phases for i -th modulation mod- i , and $\delta_i = 0$ is corresponding to an in-phase demodulation. When there is no delocation, Δ_{P2} in the above expressions disappears and both signals are maximum at the same demodulation phase, $\delta_1 = 0$ and $\delta_2 = 0$, with slight difference in absolute value. Once the DRMI is delocated, the optical phase of mod-2 inside PRC and at the detection port change relative to the non-delocated case, and both have complex values. The two signals, $\partial V_P / \partial l_P$ and $\partial V_P / \partial l_S$ are dependent on these complex parameters in different way, which result in a different optimum demodulation phases for these two.

2.4. Optimization of the delocation

A desirable situation for the l_x signal separation is that l_P and l_S signals are separated by $\pi/2$ in a demodulation phase; one of the signals disappears when the other is maximized. This is possible by a delocation, however, a delocation is an offset locking of the cavity for the mod-2, so the cavity enhancement factor decreases. This causes the reduction of the mod-2 power circulating inside the PRC, and results in a decrease in the signal strength. So there is a trade off between the signal separation angle (in demodulation phase) and the signal strength, which implies that there is some optimum delocation. The criteria for the demodulation phase was chosen so that the unwanted signal disappears, though the signal of interest is not maximal. The relation of the degree of delocation and the signal strength is shown in Figure 4. There is mild dependence on a delocation and the optimum point is around 0.05 radian. Using this optimum delocation, all of five length signals for the RSE control can be extracted from an appropriate signal ports; the results are listed in Table 2. There is still some small mixture of unnecessary signals, for example, l_- in L_- , however, as a whole the sensing matrix is almost diagonal. It is deserving special mention that three l_x signals are almost completely separated, which is a result of the delocation together with a simple design of modulation sidebands. In addition, l_- signal is available at the dark port without l_P and l_S mixture. This is because the mod-2 sideband is completely reflected from the MI and thus does not leak to the dark port. The absence of mod-2 sidebands at the dark port results in the dark port signals having no sensitivity to l_P or l_S .

3. Conclusion

A new length-sensing scheme, which makes the sensing matrix almost diagonal, is proposed for a use in a broadband RSE interferometer. The keys for an optimum diagonalization are 1) simple allocation of two sets of sidebands and 2) appropriate delocation. More detailed analysis and discussion for the scheme will appear in a separate article, however, the philosophy has been adopted as a baseline design of LCGT length sensing and control scheme.

⁶ More detailed derivation and formalism of the analytic expression will be given in separate article.

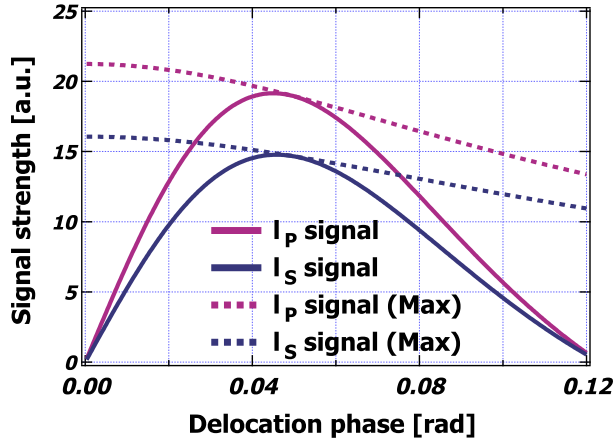


Figure 4. The variation of the signal strength depending on a delocation phase. The relevant signal is defined with the demodulation phase where an unnecessary signal disappear, so there is some optimum delocation. The dotted lines show the signal intensity with an optimum demodulation phase which maximize the signal. The decrease of the signal intensity due to delocation is several percents and not significant for diagonalization of sensing matrix.

Table 2. The length sensing matrix. The five signals corresponding to the length degrees of freedom are extracted from the appropriate signal ports (B, D, P are for bright, dark and pickoff port respectively), with suitable demodulation (SD is meant for single demodulation, and the DD for double demodulation), and with optimal demodulation phase. The numerical simulation using FINESSE software was also performed for validity conformation and the results agreed within a reasonable discrepancy which arise from the differences of resonance condition of arm cavities for modulation sidebands.

Port	Dem.	δ_1	δ_2	$\partial/\partial\Phi_+$	$\partial/\partial\Phi_-$	$\partial/\partial\phi_P$	$\partial/\partial\phi_-$	$\partial/\partial\phi_S$
V_B	SD	0	-	1	0	3.56×10^{-3}	0	2.56×10^{-3}
V_D	SD	90	-	0	1	0	1.00×10^{-3}	0
V_B	DD	0	14.4	1.00×10^{-3}	0	1	0	0
V_D	DD	90	0	0	1.00×10^{-3}	0	1	0
V_P	DD	0	42.2	1.00×10^{-3}	0	0	0	1

Acknowledgments

This research is supported in part by a Grant-in-Aid for Scientific Research on Priority Areas (415) of the Ministry of Education, Culture, Sports, Science and Technology.

- [1] J. Mizuno, K.A. Strain, P.G. Nelson, J.M. Chen, R. Schilling, A. Rüdiger, W. Winkler, and K. Danzmann, 1993 *Phys. Lett. A* **175** 273-76
- [2] Kenneth A. Strain, Guido Müller, Tom Delker, David H. Reitze, David B. Tanner, James E. Mason, Phil A. Willems, Daniel A. Shaddock, Malcolm B. Gray, Conor Mow-Lowry, and David E. McClelland, 2003 *Appl. Opt.* **42** 1244-56
- [3] J.E. Mason and P.A. Willems 2003 *Appl. Opt.* **42** 1269-82
- [4] G. Müller, T. Delker, D.B. Tanner, and D. Reitze, 2003 *Appl. Opt.* **42** 1257-68
- [5] D.A. Shaddock, M.B. Gray, C. Mow-Lowry, and D.E. McClelland, 2003 *Appl. Opt.* **42** 1283-95
- [6] O. Miyakawa, S. Kawamura, B. Abbott, R. Bork, P. Fritschel, L. Goggin, J. Heefner, A. Ivanov, F. Kawazoe, C. Mow-Lowry, A. Ourjountsev, S. Sakata, M. Smith, K. Strain, R. Taylor, D. Ugolini, S. Vass, R. Ward, and A. Weinstein, 2004 *Proceedings of the SPIE* **5500** 92-104
- [7] <http://www.rzg.mpg.de/~adf/>
- [8] R.W.P. Drever, J.L. Hall, F.V. Kowalski, J. Hough, G.M. Ford, A.J. Munley, and H. Ward, 1983 *Appl. Phys. B* **31** 97-105